ELSEVIER

Journal of Alloys and Compounds 253–254 (1997) 550–555

Journal of ALLOYS AND COMPOUNDS

Experimental analysis and modelling of the hydriding kinetics of Ni-doped and pure Mg

G. Friedlmeier*, M. Groll

Institut für Kernenergetik und Energiesysteme (IKE), University of Stuttgart, Pfaffenwaldring 31, D-70569 Stuttgart Germany

Abstract

An experimental investigation of the hydrogen absorption rate of Ni-doped and pure Mg powders is presented. The results are interpreted using a nucleation-and-growth model. Application-relevant aspects are discussed and a mathematical description of the intrinsic hydriding rate of Mg(Ni) is presented.

Keywords: Kinetics; Magnesium hydride; Absorption rate

1. Introduction

An important contribution to efficient energy usage can be provided by energy storage systems. Metal hydrides are promising materials for realising such devices [1]. The high specific hydrogen storage capacity of over 8 wt.% and the high thermodynamic stability of its hydride [2] make Mg a good candidate for thermochemical energy storage at elevated temperatures (about 300 to 500°C) [3]. The relatively slow reaction kinetics of the Mg–H system in its lower temperature range of application, however, can represent a serious technical inconvenience. Nickel was found to catalyse the hydriding and dehydriding reaction of Mg and MgH_2, respectively, and is therefore often used as an additive in order to improve the kinetic properties [4,5]. A commercially available Mg powder which was chemically doped with 2 wt.% Ni, Mg(Ni) [6], was used in a 60 MJ thermochemical energy storage system developed at IKE as a component of a small-scale solar–thermal power station [7,8]. In the following, an experimental investigation of the hydriding kinetics of Mg(Ni) and pure (undoped) Mg is presented; the results are interpreted using a nucleation-and-growth model. A mathematical description of the intrinsic hydriding kinetics of Mg(Ni) was designed suitable for computer simulation of technical reaction beds.

2. Experimental details

The experimental set-up used for the kinetic experiments is analogous to the PCI device described elsewhere [9]. At the beginning of each experiment, the sample, initially under vacuum, is suddenly put in contact with hydrogen gas at the chosen pressure (the ‘‘dead time’’ depends on the pressure level; for the conditions used here it is <4 s). The hydrogen content in the sample is determined on-line using the ideal gas equation and measuring the corresponding pressures and temperatures in an isochoric system with known volume. Due to the use of a differential pressure transducer, the system pressure changes for each experiment could be minimized (always <0.1 MPa; mostly <0.05 MPa), independent of the absolute pressure level. For this reason, most of the experiments can be considered as quasi-isobaric. Data acquisition ($\Delta t \geq 2$ s) is performed automatically by an HP 3852A datalogger connected to a PC (more details can be found in Ref. [10]).

Fig. 1 shows the reactor design. Each sample is set into a 1.65 mm wide annulus between a cylindrical stainless steel tube (∅ 13.5 mm×2.3 mm) and a coaxial sintered metal filter tube (∅ 5.6 mm×1.3 mm). A type K thermocouple (∅ 0.5 mm) set into a capillary tube (∅ 1.6 mm×0.5 mm) in direct contact with the sample allows for representative temperature measurement. The reactor is set in a high-temperature oil heat exchanger, which, using a thermostat, leads to good heat transfer characteristics. This fact, combined with the relatively slow reaction kinetics of

---

*Corresponding author.

PII S0925-8388(96)03003-4

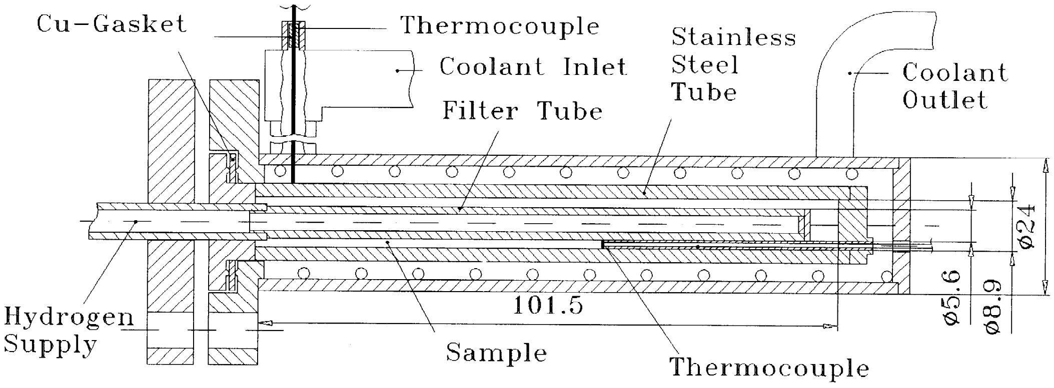

Fig. 1. Longitudinal section of the reactor.

the investigated materials in the considered temperature range (<350°C), permits the experiments to be regarded as nearly isothermal: the system pressure was always much higher than the plateau pressure corresponding to the transient sample temperature [10].

Mg and Mg(Ni) samples of 3.06 g each were investigated. Mg is a commercial 270 mesh powder (ECKA PK-31) mechanically produced by Eckart-Werke, Fürth, Germany. SEM analysis shows irregularly shaped particles with rough surfaces; laser granulometry indicates a median particle size of 56 μm [10]. Mg(Ni) consists of the same above-mentioned Mg powder which was additionally chemically doped with 2 wt.% Ni as described by Bogdanović and Spliethoff [6]. According to SEM/EDX analysis, the Ni is present as very small particles ($\varnothing \leq 3$ μm), mostly located in cracks on the Mg surface. The specific surface area of the as-delivered powders, as determined with BET surface analysis, is 0.35 and 1.38 $m^2\ g^{-1}$ for Mg and Mg(Ni), respectively [10].

Before each experiment was started, the samples were outgassed at 1 Pa and the corresponding measuring temperature for times ranging from 30 min to 24 h. No contamination-related effects of the evacuation time on the results were observed. The hydrogen gas employed was assay 99.9990% H_2.

3. Results and discussion

3.1. Absorption experiments with Mg(Ni) and Mg

Figs. 2 and 3 show absorption experiments with Mg(Ni) for different pressures at $\vartheta_o = 270$°C and 343°C, respectively. These results show characteristics which are qualitatively analogous to the ones already reported for pure Mg [11]: (a) For hydrogen pressures p close to the plateau pressure p_{Pl} (such as 0.65, 0.69 and 0.74 MPa at 343°C, where $p_{\mathrm{Pl}} = 0.55$ MPa), sigmoidal $\xi = \mathrm{f}(t)$ hydriding curves are measured ($\xi = x/x_{\mathrm{stoich}}$ is the degree of hydriding, with x as the measured hydrogen content and x_{stoich} as the content corresponding to the expected stoichiometry); (b) For sufficiently high pressures (such as 1.01 and 1.30 MPa at 343°C), curves with continuously decreasing reaction rates are measured; (c) The higher the hydrogen pressure, the faster the hydriding reaction starts, but, if a

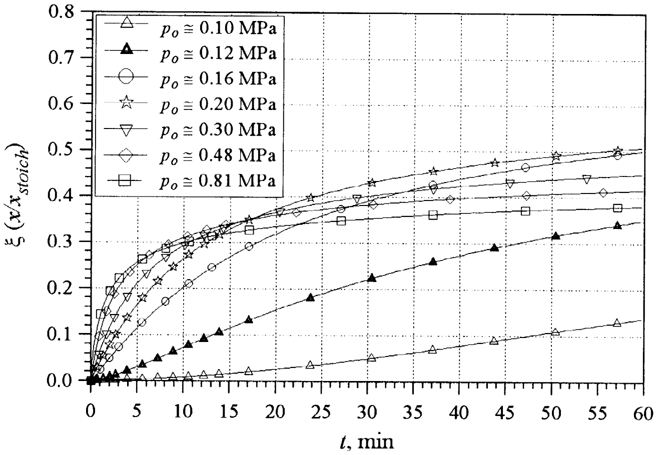

Fig. 2. Hydriding experiments with Mg(Ni) at $\vartheta_o = 270$°C and different pressures.

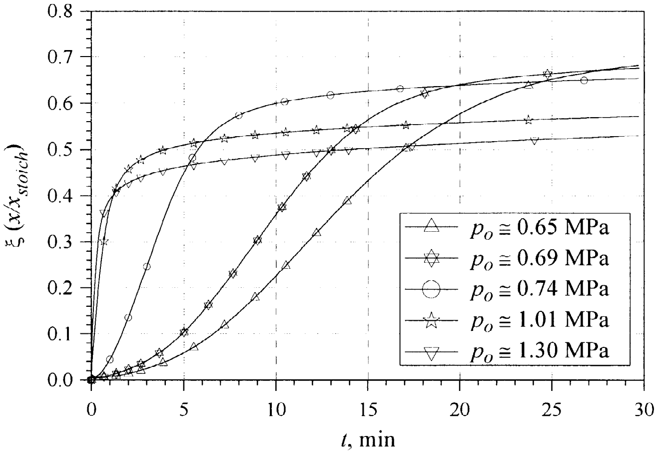

Fig. 3. Hydriding experiments with Mg(Ni) at $\vartheta_0 = 343$°C and different pressures.

sufficiently long period of time is considered, higher hydriding degrees are achieved for lower pressures. This effect leads to a crossing of the $\xi = f(t)$ curves which is not observed for most hydride materials and has important practical consequences (see below).

Fig. 4 compares analogous absorption experiments with Mg(Ni) and undoped Mg for various pressures at $\vartheta_0 =$ 321°C. These results show another interesting feature: Mg(Ni) hydrides faster during an initial phase, but after a given time the hydriding curves $\xi = f(t)$ of Mg(Ni) and Mg cross each other, leading to higher hydriding degrees for Mg if sufficiently long periods of time are considered, a result which also has technical importance.

3.2. Nucleation-and-growth model

The above-described results can be explained with a nucleation-and-growth model. It is supported by various experimental results on the Mg–H system reported in the literature and was first suggested in a similar form for pure Mg by Isler [11].

Optical microscopy [11], SEM [11–14] and TEM [15] of Mg powders, chips and foils in different hydriding stages show the following characteristics: (a) The hydride phase nucleates as isolated grains on the particle surface; (b) These grains grow in three dimensions, viz. approximately in the form of semi-spheres, into the bulk. Grain boundaries in the α-phase (Mg) do not affect the growth of the β-phase (MgH_2); (c) The density of β-nuclei on the surface increases with pressure; (d) At high pressures (and long times) partially hydrided particles show a closed external hydride layer covering a metallic core. Fig. 5 visualizes these experimental observations. Further literature data [16,17] indicate that the hydrogen diffusion rate in β-MgH_2 is many orders of magnitude lower than in α-Mg.

Assuming that the reported results are also valid for Mg(Ni), a self-consistent model can be postulated which explains the hydriding behaviour of Mg(Ni) observed in Figs. 2–4: (a) For hydrogen pressures close to p_{Pl}, the chemical reaction, which is proportional to the α–β phase boundary area, is the rate-controlling reaction step. This explains the sigmoidal shape of the $\xi = f(t)$ curves [18,19]. Since only a few hydride grains nucleate, they can grow

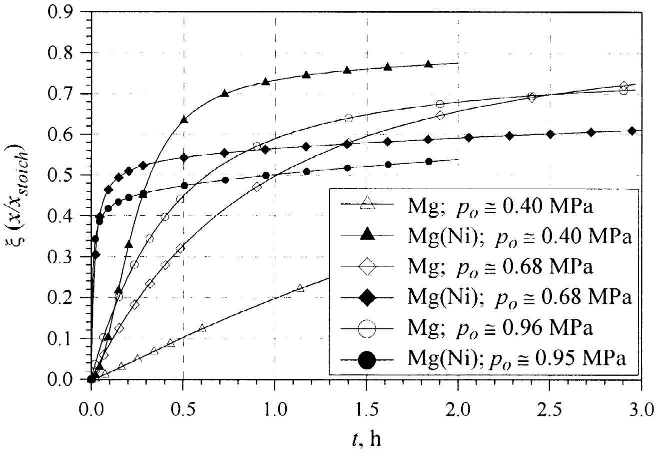

Fig. 4. Hydriding experiments with Mg(Ni) and Mg at $\vartheta_0 = 321$°C and different pressures.

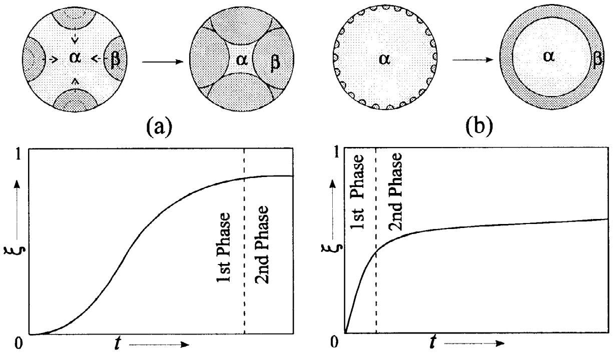

Fig. 5. Cross-section of a Mg or Mg(Ni) particle at two different times and typical $\xi = \mathrm{f}(t)$ curves for hydriding at $p \approx p_{\mathrm{Pl}}$ (a) and $p \gg p_{\mathrm{Pl}}$ (b) (schematic).

large before a completely closed hydride layer is formed on the particles—large hydride grains lead to high hydriding degrees. Hydrogen diffusion takes place either through the α-phase or through the α–β phase boundary. Once the hydride layer has closed, the reaction nearly stops owing to the impermeability of this layer. The extremely slow mass transport (diffusion) through this layer is now the rate-controlling reaction step; (b) For high hydrogen pressures, instead, a larger amount of hydride grains nucleate. Owing to geometrical reasons they can grow less, as compared to (a), before a closed hydride layer is formed and the reaction practically stops (diffusion-controlled step). The first reaction phase is in this case most probably surface-controlled (chemisorption). The latter assumption is supported by the proportionality of the reaction rate with the pressure difference ($p_{\mathrm{H}_2} - p_{\mathrm{Pl}}$) observed for this case [20] (see below). The chemical reaction can be excluded since no sigmoidal curves are measured. Diffusion control would lead to a two-dimensional hydride growth on the particle surface, where the transport paths are shorter. This, however, contradicts the microscopic observations of three-dimensional hydride grain growth mentioned above.

The (mainly quantitative) differences between the hydriding curves of Mg(Ni) and pure Mg shown in Fig. 4 can also be explained with this model: (a) For similar pressure and temperature conditions, Mg(Ni) starts hydriding faster, but Mg can be hydrided to a higher degree before a diffusion control starts because less hydride grains nucleate for the latter, indicating that Ni catalyses the nucleation process; (b) The fact that the transition of sigmoidal $\xi = \mathrm{f}(t)$ curves to ones with a continuously decreasing reaction rate occurs at higher pressure differences for Mg(Ni) than for Mg can be explained by a Ni-catalysed chemisorption. For Mg(Ni), chemisorption is fast and the comparatively slow chemical reaction limits the reaction. For Mg, chemisorption is much slower and limits the reaction, leading to hydriding curves with a continuously decreasing rate. The chemical reaction becomes rate-controlling only for pressures very close to p_{Pl}.

3.3. Practical consequences of the hydriding results

As mentioned above, the results shown here have technical importance: (a) If high hydriding degrees of Mg(Ni) are desired, hydriding at conditions far from equilibrium or at high initial rates should be avoided, in order to avoid fast hydride nucleation and therefore premature closure of the hydride layer on the powder particles. High initial rates should be allowed only when they have priority over total achievable capacity before the very slow diffusion-controlled reaction phase starts; (b) Ni catalysis is advantageous only when high initial rates have priority over total achievable capacity. Otherwise it has a negative effect. (Additional results not presented here indicate that the catalytic effect of Ni becomes negligible, and therefore technically unnecessary, for temperatures higher than 400°C. Below 300°C, however, the catalytic effect is strong and can be considered as advantageous for most practical uses [10].)

4. Mathematical description of the intrinsic hydriding kinetics of Mg(Ni) for $p \gg p_{\mathrm{pl}}$

In this section a mathematical description of the intrinsic hydriding kinetics of Mg(Ni) is presented for $p \gg p_{\mathrm{Pl}}$ which is suitable for computer simulation of the behaviour of technical reaction beds and devices based on this material. Experiments with (large) technical reaction beds have shown that in this case hydriding practically always becomes limited by heat transfer [21]. Since for such conditions the system behaviour is independent of the intrinsic reaction kinetics, the latter does not need to be known. This, however, is not true for two reaction phases: (a) the initial ‘‘warming-up’’ phase, while the system and plateau pressures have not yet equalized; and (b) the final, diffusion-controlled reaction phase. For the latter, no systematic dependence of the reaction rate $\nu = \mathrm{d}\xi/\mathrm{d}t$ on pressure, temperature and ξ was observed; very low ν values between 0.5 and $2 \times 10^{-5}\ \mathrm{s}^{-1}$ were measured.

The ‘‘warming-up’’ phase will normally be the longer, the larger the initial pressure difference ($p - p_{\mathrm{Pl}}$) is. For small pressure differences, heat transfer will quickly control the reaction, so that a minimum effect of the intrinsic kinetics on the system behaviour is expected. From an application point of view (i.e. for computer simulations), therefore, only a mathematical description of the kinetics for the initial reaction phase for $p \gg p_{\mathrm{Pl}}$ is needed. This will be done in the following. In this treatment isothermal and isobaric conditions are assumed.

Fig. 6 shows the reaction rate ν as a function of the hydriding degree ξ for various pressures and temperatures. A linear dependence of ν on ξ during the first reaction phase can be clearly observed. This led us to postulate a similar rate equation to the one Isler [11] found to describe his results for pure Mg:

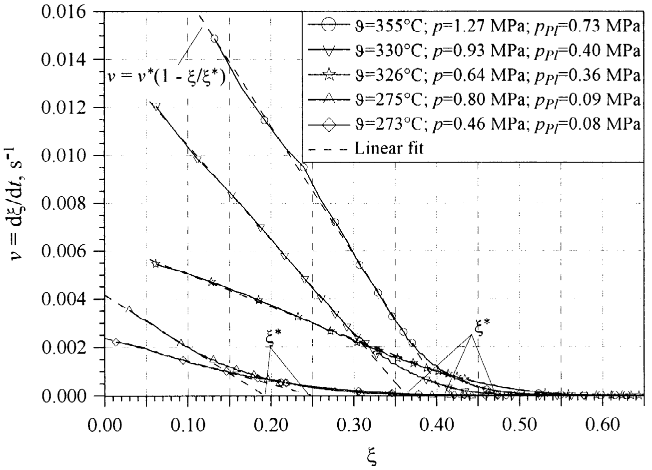

Fig. 6. Reaction rate vs. hydriding degree for Mg(Ni) at different temperatures and pressures [$\nu^* = \nu/(1-\xi/\xi^*)$].

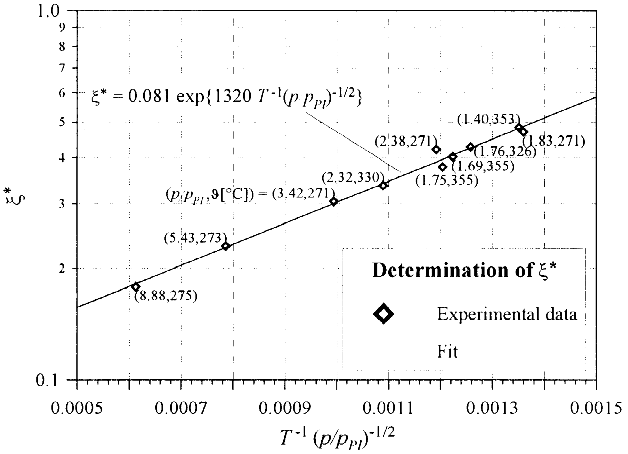

Fig. 8. Determination of the temperature and pressure dependence of ξ^* (see Fig. 6).

$$\nu(p, T, \xi) = k_f \left(1 - \frac{\xi}{\xi^*(p, T)}\right)(p_{H_2} - p_{Pl})\exp\left(\frac{-E_a}{k_B T}\right), \tag{1}$$

where k_f is the proportionality factor, k_B is the Boltzmann constant and E_a is the activation energy of the rate-controlling reaction step; ξ^* represents approximately the degree of hydriding at which the reaction starts to be diffusion-controlled. Eq. (1) is based on two main assumptions: (a) the reaction is surface-controlled (chemisorption) and therefore $\nu \propto (p - p_{Pl})$ [20]; and (b) the reaction is thermally activated and therefore the temperature dependence of ν can be described with an exponential Arrhenius factor. This model describes very well the hydriding behaviour of Mg(Ni), as is demonstrated by the high linearity of the experimental data on the Arrhenius plot (Fig. 7). Fitting the data to Eq. (1) led to values of 12 800 s^{-1} MPa^{-1} and 1.1×10^{-19} J for k_f and E_a, respectively. Comparison of this result with literature data for Mg ($E_a = 1.6 \times 10^{-19}$ J [11]) indicates that the activation energy of chemisorption has been reduced here by the catalytic effect of Ni.

Still to be solved remains the problem of predicting the value of ξ^* representing the hydriding degree at which the first reaction phase ends (i.e. the diffusion control starts). As is visible from Fig. 6, it can take completely different values depending on p and T. Fig. 8 shows that all measured data can be excellently approximated with the following empirical equation:

$$\xi^*(p, T) = 0.081 \exp\left(\frac{1\,320\text{ K}}{T(p/p_{Pl})^{1/2}}\right) \quad (270 \leq \vartheta \leq 350°\text{C}) \tag{2}$$

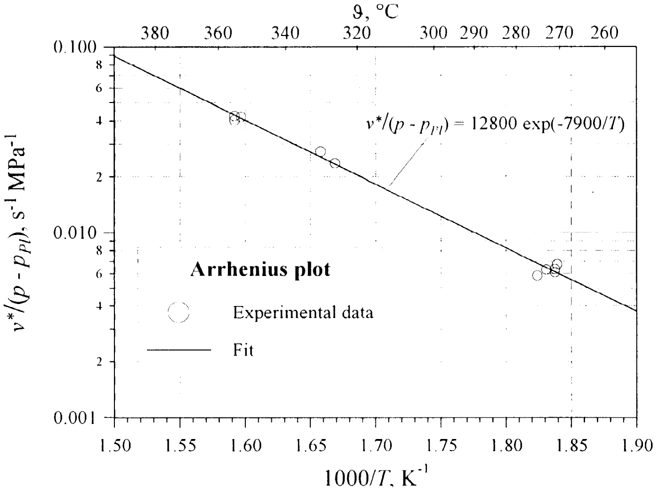

Fig. 7. Arrhenius plot for the first hydriding phase of Mg(Ni). Chemisorption is assumed to be rate-controlling [$\nu^* = \nu/(1-\xi/\xi^*)$].

Since ξ^* is closely related to the nucleation process (high values of ξ^* correspond to low nucleation rates), this result suggests that the ratio p/p_{Pl} rather than the pressure difference $(p-p_{\mathrm{Pl}})$ governs the nucleation process. This result also has technical importance and explains why higher degrees of hydriding (i.e. values of ξ^*) can in general be achieved for increasing temperatures if experiments with nearly constant values of $(p-p_{\mathrm{Pl}})$ are compared [10] (notice that, for the conditions used here, the factor $T(p/p_{\mathrm{Pl}})^{1/2}$ decreases with increasing T due to the temperature dependence of p_{Pl}).

5. Conclusions

The hydriding behaviour of Mg(Ni) and Mg shows a complex dependence on pressure and temperature. This behaviour can be well explained by a nucleation-and-growth model. High nucleation rates lead to a premature standstill of the reaction, making complete hydriding practically impossible. In order to achieve high conversion degrees, hydriding should be performed at conditions close to equilibrium ($p \approx p_{\mathrm{Pl}}$). Between about 300 and 400°C the catalytic effect of Ni on the Mg–H_2 reaction is positive only if high initial reaction rates have priority over the (in technically reasonable times) achievable maximum hydriding degree. Otherwise the effect of Ni is negative. A mathematical description of the initial hydriding rate of Mg(Ni) for $p \gg p_{\mathrm{Pl}}$ has been presented. Indications were found that the nucleation process of the hydride phase is governed mainly by the pressure ratio p/p_{Pl}.

Acknowledgments

This work was financially supported by the Deutsche Forschungsgemeinschaft (DFG) in the frame of Sonderforschungsbereich 270 and the Bundesministerium für Bildung, Wissenschaft, Forschung und Technologie (BMBF) of Germany under Contract No. 0328939B.

References

[1] G. Sandrock, S. Suda and L. Schlapbach, in L. Schlapbach (ed.), *Hydrogen in Intermetallic Compounds II, Topics in Applied Physics*, Vol. 67, Springer, Berlin, 1992, Chap. 5.
[2] J. Stampfer Jr., C. Holley Jr. and J. Suttle, *J. Am. Chem. Soc., 77* (1960) 3504.
[3] H. Buchner, *Energiespeicherung in Metallhydriden*, Springer, Wien, 1982, Chap. 2.
[4] J.J. Reilly and R. Wiswall Jr., *Inorg. Chem., 7* (1968) 2254.
[5] N. Gérard and S. Ono, in L. Schlapbach (ed.), *Hydrogen in Intermetallic Compounds II, Topics in Applied Physics*, Vol. 67, Springer, Berlin, 1992, Chap. 4.
[6] B. Bogdanović and B. Spliethoff, *Int. J. Hydrogen Energy, 12* (1987) 863.
[7] M. Wierse, R. Werner and M. Groll, *J. Less-Comm. Metals, 172–174* (1991) 1111.
[8] M. Wierse and M. Groll, *Proc. 11th WHEC, Stuttgart, June 23–28, 1996*.
[9] G. Friedlmeier, M. Schaaf and M. Groll, *Z. Phys. Chem., 183* (1994) 185.
[10] G. Friedlmeier, Charakterisierung von Hochtemperatur-Metallhydriden auf Magnesium-Basis, *PhD Thesis*, University of Stuttgart, 1997, (in preparation).
[11] J. Isler, Étude Cinétique des Reactions d'Hydruration et de Déshydruration du Magnésium et du Mélange Mg–($LaNi_5$), *PhD Thesis*, University of Dijon, 1979.
[12] J. Isler, E. Joly, A. Barbet and N. Gérard, *Compt. Rend. Acad. Sci. Paris, Sér. C, 290* (1980) 317.
[13] A. Pedersen, J. Kjøller, B. Larsen and B. Vigeholm, *Int. J. Hydrogen Energy, 10* (1985) 851.
[14] A. Pedersen, K. Jensen, B. Larsen and B. Vigeholm, *J. Less-Comm. Metals, 131* (1987) 31.
[15] T. Schober, *Metall. Trans. A, 12* (1981) 951.
[16] J. Töpler, H. Buchner, H. Säufferer, K. Knorr and W. Prandl, *J. Less-Comm. Metals, 88* (1982) 397.
[17] J. Renner and H. Grabke, *Z. Metallkd., 69* (1978) 639.
[18] L. Harrison, in C. Bamford and C. Tipper (eds.), *Chemical Kinetics, The Theory of Kinetics*, Vol. 2, Elsevier, Amsterdam, 1969, Chap. 5.
[19] Ch. Gommel, Messungen zur Kinetik der Wasserstoffaufnahme von $LaNi_{4.7}Al_{0.3}$ und Mg(Ni) und Modellrechnungen zur Reaktionskinetik von Hydridspeichermaterialien, *Diploma Thesis*, University of Stuttgart, IKE-Report 5D-211, 1993.
[20] G. Hörz, in E. Fromm and E. Gebhardt (eds.), *Gase und Kohlenstoff in Metallen*, Springer, Berlin, 1976, Chap. B.
[21] P. Spoerel, Experimente mit technischen Magnesiumhydrid-Reaktionsbetten, *Diploma Thesis*, University of Stuttgart, IKE-Report 5D-271, 1996.